A New Lower Limit for the Ultimate Breaking Strain of Carbon Nanotubes

Chia-Chi Chang,[†] I-Kai Hsu,[‡] Mehmet Aykol,[§] Wei-Hsuan Hung,[‡] Chun-Chung Chen,[§] and Stephen B. Cronin[†,§,*]

[†]Department of Physics, [‡]Department of Materials Science, and [§]Department of Electrical Engineering, University of Southern California, Los Angeles, California 90089

ABSTRACT We apply immense strain to ultralong, suspended, single-walled carbon nanotubes while monitoring their Raman spectra. We can achieve strains up to 13.7 ± 0.3% without slippage, breakage, or defect formation based on the observation of reversible change in Raman spectra. This is more than twice that of previous observations. The rate of G band downshift with strain is found to span a wide range from −6.2 to −23.6 cm^{-1}/% strain. Under these immense strains, the G band is observed to downshift by up to 157 cm^{-1} (from 1592 to 1435 cm^{-1}). Interestingly, under these significant lattice distortions, we observe no detectable D band Raman intensity. Also, we do not observe any broadening of the G band line width until a threshold downshift of $\Delta\omega_G > 75$ cm^{-1} is achieved at high strains, beyond which the fwhm of the G band increases sharply and reversibly. On the basis of a theoretical nonlinear stress−strain response, we estimate the maximum applied stress of the nanotubes in this study to be 99 GPa with a strength-to-weight ratio of almost 74 000 kN · m/kg, which is 30 times that of Kevlar and 117 times that of steel.

KEYWORDS: Raman · strain · CNTs · individual · strength · stress · CVD

Carbon nanotubes present a unique mechanical system that is harder than diamond in the axial direction ($Y = 0.97$TPa) yet extremely flexible in the transverse direction.[1,2] Unlike diamond, however, carbon nanotubes are not brittle and can be elongated considerably before breaking.[3] Nanotubes' tremendous strength-to-weight ratio has been explored for a number of applications including electromechanical resonators with attoNewton (10^{-18} N) and zeptogram (10^{-17} g) sensitivity,[4,5] high strength, lightweight composites,[6,7] and even space elevators.[8,9] However, the exceptional mechanical properties of nanotubes have been difficult to realize experimentally and utilize for practical applications, mainly because the strength of the nanotube interface has been the limiting factor.

For more than 10 years, theoretical calculations of carbon nanotubes under stain have predicted the formation of 5−7 defects for strains above 6%.[10] Several experimental groups corroborated these predictions, observing breaking strains of 5.3 and 5.8%.[11,12] However, a few years later, revised theoretical calculations reported that nanotubes should be stable against defect formation beyond strains of 15%.[13] They calculated an activation barrier for 5−7 defect formation of 2 eV at 15% strain, making nanotubes very stable against defect formation at room temperature. The authors stated that the "ultimate strength limit of carbon nanotubes has yet to be reached experimentally".[13] It is likely that these early experimental measurements merely reflected the strength of the nanotube−substrate contact and, hence, represent only a lower limit of the true breaking strain of carbon nanotubes.

Several research groups have performed Raman measurements of nanotubes under strain. In a majority of this previous work,[6,7,14−19] bulk quantities of nanotubes dispersed in polymer composites were measured simultaneously, giving an ensemble average of many nanotubes. These measurements indicated that only a small fraction of the strain applied to the composite was transferred to the nanotubes within the composite. In later measurements, individual nanotube bundles were measured under strain.[20−23] These studies showed that only 10% of the applied strain was transferred to the individual nanotubes within the bundle and that the primary effect of the strain was to debundle the nanotubes.[22] As a result of this reduced transfer of strain, previous experimental studies have not been able to provide sufficient strains to achieve mechanical breakdown in nanotubes.

RESULTS AND DISCUSSION

According to SEM images (Figure 1), the density of nanotubes is around 1 per

*Address correspondence to scronin@usc.edu.

Received for review April 30, 2010 and accepted July 30, 2010.

Published online August 10, 2010. 10.1021/nn100946q

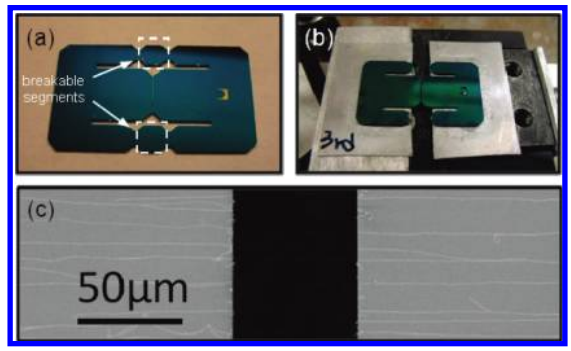

Figure 1. Photograph images of our experimental setup and SEM images of suspended SWCNTs: (a) breakable H-chip, (b) broken H-chip with suspended SWCNTs mounted on the translation stage, and (c) SEM image of SWCNTs spanning a trench.

10 μm separation, although they sometimes form small bundles. The small laser spot size (0.4 μm) and sharp Raman signals indicate that only one nanotube contributes to the data in each measurement. The long nanotube−substrate contact length is essential to achieving large strains in nanotubes. Son *et al.* determined the frictional force between a nanotube and its underlying Si/SiO_2 substrate to be 10 pN/nm. This relatively small frictional force per unit length, integrated over these long lengths, yields large net strains.[26] For every 1 μm of nanotube−substrate contact length, up to 10 nN can be exerted without slippage. Assuming a diameter of 1 nm, this corresponds to approximately 10 GPa per 1 μm of contact length. Using this technique, we are able to achieve sufficient strains in carbon nanotubes, far exceeding those of previous reports, which were limited by the effects of nanotube−substrate slippage and nanotube debundling.

Spatial mapping of these Raman spectra allows us to find the angle between the nanotube and the direction of strain, θ, and determine a more accurate value of strain by the relation $\varepsilon = \Delta L \cos\theta / L$, where L is the initial length of suspended SWCNTs and ΔL is the length change due to strain. Also, we find that suspended SWCNTs grown by the high flow rate method lie straight across the trench with very little slack. We quantify the amount of slack by monitoring the G band Raman shift. Typically, during the first few displacements of the translation stage, we observe no downshift of the G band mode, as the slack is taken up. Once a downshift is observed, we define this as 0% strain. From this point on, Raman spectra are used to ensure that only reversible changes occur in the nanotube. In these samples, the nanotubes lie on SiN-coated silicon substrates, which produce a strong background signal that obscures the relatively small nanotube signals. By checking that the 0% strain spectrum remains the same before and after applying strain, we carefully rule out any possible slippage of the nanotubes on the underlying substrate, as observed previously by Kumar *et al.*[22] In each strain cycle, the strain was incrementally increased while checking that the slack spectra remained unchanged. The last data point taken before an irreversible change is observed is defined as the maximum applied strain (ε_{max}). It should be noted, however, that ε_{max} is a lower limit of the actual breaking strength of the nanotube since the irreversible changes observed here correspond to slippage events rather than breakage of the nanotubes, as evidenced by the presence of a Raman signal, as described below.

Figure 2a plots the G band frequency as a function of strain, showing a strain-induced downshift rate of −6.2 cm^{-1}/% strain. This downshift is remarkably linear with strain and is understood on the basis of weakening of the carbon−carbon bonds, which lowers their vibrational frequency. Several data sets depicting stretching and relaxing of the nanotube show consistent and reversible data in which the G band frequency reverts to its original prestrain position after the strain is relaxed. This indicates that the nanotube was able to endure these enormous strains without breaking, forming 5−7 defects, or slipping on the underlying SiN substrate, which would result in irreversible shifts in the Raman frequency. Figure 2b shows the G band Raman spectra of the nanotube before, during, and after applying 12% strain. Before applying strain, the Raman spectrum shows a single, sharp G band peak, signifying that this is a semiconducting nanotube.[28] No D band was observed for this nanotube, even at large applied strains, indicating that there are very few defects in this nanotube.[29] At 12% strain, the spectrum shows two peaks at 1490 and 1580 cm^{-1}. The 1490 cm^{-1} peak is attributed to the G_- Raman mode, while the 1580 cm^{-1} peak is attributed to amorphous carbon since it does not respond to strain at all. Remarkably, after such a large distortion of the lattice, the G band reverts back to its original prestrain line shape and frequency. Figure 2c shows the Raman intensity plotted as a function of Raman shift (cm^{-1}) and strain (%). Here, the continuous modulation of the G band peak can be seen clearly, varying all the way down to 1487 cm^{-1}. Our last data point was taken at a strain of 13.7%. Beyond this strain, the G band shifted back to 1567 cm^{-1}, indicating that the nanotube slipped off the substrate but was not broken. Figure 2d shows the G band line width under the applied strains. Here, we have plotted the fwhm as a function of the G band downshift. We see essentially no change in the line width until a downshift of 75 cm^{-1}, which corresponds to a strain of 9.5%. Beyond this threshold, we observe a sharp increase in the fwhm of this Raman mode. Somewhat surprisingly, the fwhm reverts back to its original prestrain line width after relaxing the applied strain, indicating that no permanent defects or damage have been induced in the nanotube.

Figure 3 shows the data from another suspended, ultralong CNT across a 170 μm wide slit. While this sample could only endure strains of 6.2%, we observe a much higher rate of G band downshift with strain

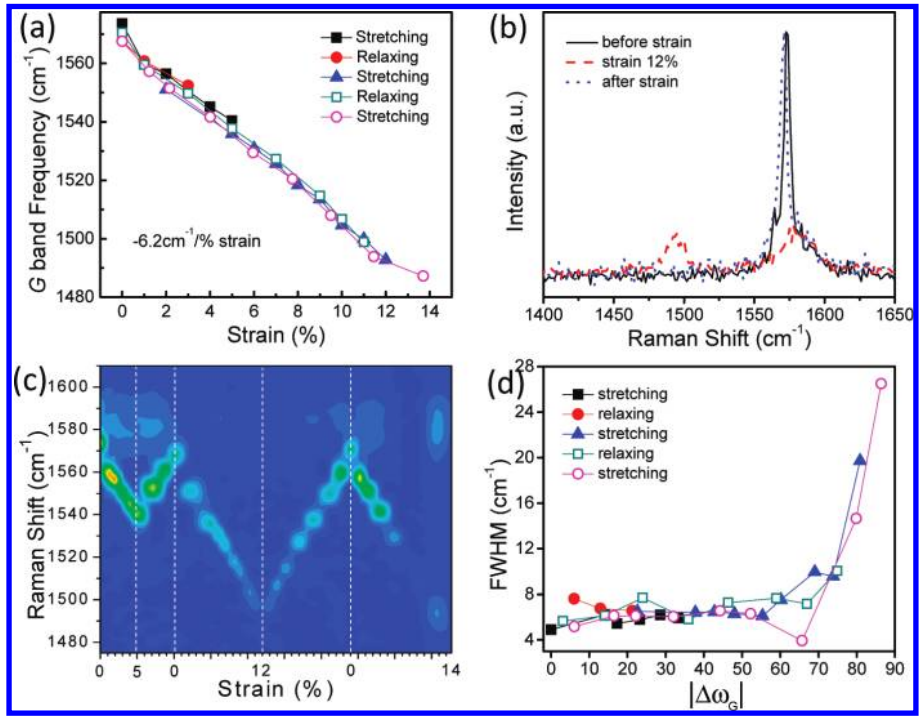

Figure 2. (a) G band Raman frequency of an individual, suspended carbon nanotube under applied strain. (b) Raman spectra before, during, and after applying 12% strain. (c) Raman spectra (vertical axis) mapped chronologically as the sample is strained and unstrained. (d) Full width at half-maximum plotted as a function of G band downshift, $|\Delta\omega_G|$.

(−23.6 cm^{-1}/% strain), resulting in a maximum G band downshift of 157 cm^{-1} (from 1592 to 1437 cm^{-1}). Figure 3a shows the G band frequency plotted as a function of strain. Again, several data sets depicting stretching and relaxing of the nanotube show reversible (elastic) changes in the G band, indicating no occurrence of defect formation or slippage. The raw Raman spectra taken before, during, and after 6.2% strain are shown in Figure 3b. Here, two peaks can be seen in the spectra, corresponding to G_+ and G_-. Figure 3c shows the Raman spectra mapped as a function of strain. The G_+ and G_- bands here downshift at different rates of −10.8

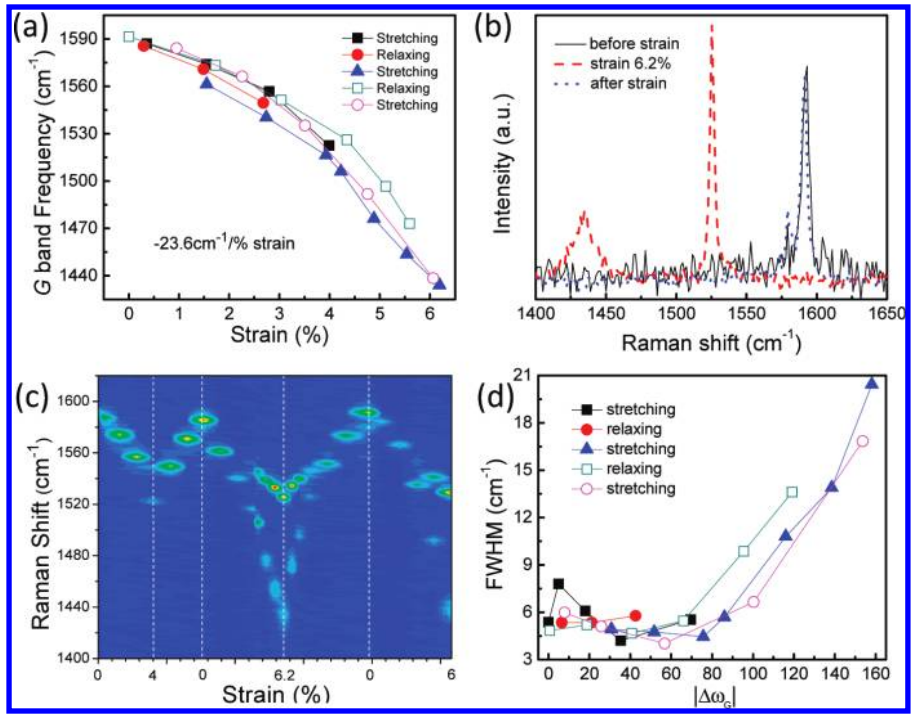

Figure 3. (a) G band Raman frequency of another suspended carbon nanotube under applied strain. (b) Raman spectra before, during, and after applying 6.2% strain. (c) Raman spectra (vertical axis) mapped chronologically as the sample is strained and unstrained. (d) Full width at half-maximum plotted as a function of G band downshift, $|\Delta\omega_G|$.

TABLE 1. Summary of Raman Data Taken on Nanotubes under Strain

sample	d_B (nm)	L (μm)	$\Delta\omega_{max}$ (cm^{-1})	$d\omega/d\varepsilon$ (cm^{-1}/%)	ε_{max} (%)	tensile stress (GPa)
#1_suspend		62	68 (1583−1515)	−17	4 ± 0.8	38.1
#2_suspend		98	32 (1591−1559)	−10.6	3 ± 0.5	29.3
#3_suspend	1.3	42	51 (1582−1531)	−6.5	8.3 ± 1.2	70.6
#4_suspend	3.3	59	47 (1575−1528)	−6.9	6.8 ± 0.8	60.2
#5_suspend		174	157 (1592−1435)	−10.8/−23.6	6.2 ± 0.3	55.8
#6_suspend	3.4	195	86 (1573−1487)	−6.2	13.7 ± 0.3	98.9

and −23.6 cm^{-1}/% strain, respectively. These differing rates of downshift with strain were predicted theoretically[30,31] and were also observed expermentally,[32] as described below. The G band line width, plotted in Figure 3d, shows no change until a downshift of 80 cm^{-1} (4% strain) is achieved, above which the fwhm increases sharply, but reversibly. Upon relaxation of this strain, both the frequency and line width of the G band revert back to their prestrain conditions. No D band was observed in either of the nanotubes shown in Figures 2 and 3 during the course of these measurements.

The deviation of the data points taken at 0% strain in Figure 2a is due to the poor mechanical precision of translation stage, rather than irreversible changes in the nanotube. In Figure 3a, the different data sets deviate significantly from each other due to the large downshift rate of −23.6 cm^{-1}/% strain as compared to that in Figure 2a, which is only −6.2 cm^{-1}/% strain. Therefore, in Figure 3a, a relatively small uncertainty in strain results in a large variation in the G band frequency.

On the basis of our observations, the Raman intensity also changes with applied strain. Figure 2c shows the Raman intensity drop by a factor of 19 at 13.7% strain, due to the strain-induced change in the electronic transition energy of the nanotube.[27,33−40] This shifts the resonance window of the nanotube away from the laser energy. Since the strain-induced shift depends strongly on chiral angle, a 13.7% strain can shift the electronic transition energy by anywhere between 0 and 760 meV.[27] Therefore, the 19-fold decrease in Raman intensity observed for the nanotube in Figure 2 is reasonable. The nanotube in Figure 3 shows a weaker strain dependence of the Raman intensity on strain, implying that the chiral angle of this nanotube is closer to 30°.[27,33]

Table 1 summarizes the results observed in six suspended nanotube samples strained in this way. The table lists the diameter of the nanotube/bundle as determined by atomic force microscopy (AFM) (d_B), the initial length of the unstrained suspended segment of the nanotube (L), the maximum observed downshift of the Raman frequency ($\Delta\omega_{max}$), the rate of downshift with strain ($d\omega/d\varepsilon$), the maximum strain observed (ε_{max}), and the estimated tensile stress corresponding to the maximum observed strain. On the basis of previous experimental[41] and theoretical[42] reports on the nonlinear stress−strain behavior of carbon-based materials, a quadratic function was used to represent the nonlinear stress−strain behavior, in which $\sigma = A\varepsilon + B\varepsilon^2$, where σ is the stress in units of GPa, ε is the dimensionless applied strain, A is the Young's modulus in units of GPa, and B is the third-order elastic modulus in units of GPa. Liu *et al.*[42] have used *ab initio* methods to calculate coefficients of $A = 1047.3$ GPa and $B = -2375.2$ GPa. The maximum applied stresses of our nanotubes were obtained using these coefficients and our maximum applied strain values in this equation. Again, our samples exhibited partial slippage of the nanotube between 3 ± 0.5 and 13.7 ± 0.3% strain. That is, we observe a relaxation of strain, but the nanotube was still suspended. The large variation of observed maximum strain results from the different contact length and contact quality from sample to sample.

In Table 1, the rate at which the G band downshifts with strain ($d\omega/d\varepsilon$) spans a wide range from −6.2 to −23.6 cm^{-1}/% strain for different nanotubes measured in this study. Using molecular dynamics simulations, Yang *et al.* have predicted a strong chirality dependence of the rate of G band downshift with strain, ranging from −6.25 to −27.5 cm^{-1}/% strain.[30] Similar results were also observed by Wu *et al.* using *ab initio* method[31] and by *Gao et al.* experimentally.[32] This range is in excellent agreement with our experimental results. In particular, they found strain-induced downshifts of $\partial\omega_{G+}/\partial\varepsilon = -8$ cm^{-1}/% strain and $\partial\omega_{G-}/\partial\varepsilon = -24$ cm^{-1}/% strain for armchair nanotubes (n,n), and $\partial\omega_{G+}/\partial\varepsilon = -25$ cm^{-1}/% strain and $\partial\omega_{G-}/\partial\varepsilon = -10$ cm^{-1}/% strain for zigzag nanotubes (n,0).[30] However, they only performed calculations on these highly symmetric armchair (n,n) and zigzag (n,0) nanotubes, which have relatively few atoms per unit cell compared to achiral nanotubes. Nevertheless, we can estimate the approximate chirality from the relative downshifts of the G_+ and G_- band Raman modes. For the nanotube in Figure 3, $\partial\omega_{G+}/\partial\varepsilon < \partial\omega_{G-}/\partial\varepsilon$, indicating that its chirality is close to that of an armchair nanotube ($\theta \approx 30°$). Since the downshift in the G band frequency gives a measure of the weakening of the C−C bond, it is reasonable to expect breakage to occur at similar G band downshifts rather than similar values of strain. The line width data (Figures 2d and 3d) further support this notion, showing thresholds for line width broadening that occur at similar G band downshifts, rather than strain. Since we do not see any evidence of defect formation

in these nanotubes, it is not clear from our data whether these maximum applied strains (ε_{max}) were limited by slippage or indicate the true threshold strain for mechanical breakdown. While sample #6 exhibited a maximum strain of 13.7 $\pm$ 0.3%, we believe that the lower values of maximum strain observed in the other nanotube samples are due to slippage between the nanotubes and their underlying substrates since a Raman signal can still be observed from the nanotubes after the maximum strain is reached. We, therefore, ascribe the ε_{max} values given in Table 1 as lower limits for the ultimate strength of carbon nanotubes. Four out of the six nanotubes in this study have relatively low initial G band frequencies (1573−1583 cm^{-1}). We have ruled out the possibility of prestrain induced during the nanotube growth process by making the nanotubes slack and verifying that no further upshift occurs. In a previous publication, we reported laser heating of suspended carbon nanotubes,[43] which required laser powers higher than 3 mW focused to a 0.4 μm spot size in order to observe G band downshifts due to laser heating of the nanotube. We are, therefore, confident that laser heating can be ignored in the work presented here.

CONCLUSIONS

In conclusion, by growing ultralong carbon nanotubes with long substrate−nanotube contacts, we have been able to apply immense strains to individual, suspended carbon nanotubes. Monitoring the Raman spectra while reversibly straining and relaxing the nanotube enables us to identify and quantify the effects of slippage, which have limited the strain achieved in previous measurements. No evidence of defect formation was observed under strains up to 13.7 $\pm$ 0.3%. This is twice the value of strain achieved in previous measurements, establishing a new lower limit for the ultimate strength of carbon nanotubes. The rates of G band downshift with strain span a large range from −6.2 to −23.6 cm^{-1}/% strain, which is consistent with theoretical predictions and previous observation. Line width broadening is observed with strains beyond a threshold downshift of the G band of $\Delta\omega_G > 75$ cm^{-1}. Beyond this, the fwhm of the G band increases sharply and reversibly.

METHODS

Breakable H-Chip Fabrication. An H-shaped pattern is etched through a double-sided SiN/Si/SiN wafer, as shown in Figure 1. A breakable segment of the chip, consisting of partially etched Si, enables the two sides of the slit to be separated easily after they have been mounted on a translation stage equipped with half micrometer step resolution (Figure 1b). That gives up to 0.25% strain resolution in long suspended nanotubes (195 μm). This technique is very similar to the sample fabrication developed by Huang *et al.*[27]

Carbon Nanotube Growth. Ultralong suspended single-walled carbon nanotubes are grown across the slit by chemical vapor deposition following the general procedure reported by Brintlinger,[24,25] as shown in Figure 1c. We use ferric nitrate, $Fe(NO_3)_3$, catalyst and flow H_2:CH_4:C_2H_4 at rates of 1500:1500:50 sccm at 900 °C for 25 min.

Raman Spectroscopy. A Renishaw *inVia* micro-Raman spectrometer is used to take Raman spectra of these individual nanotubes under various degrees of applied strain with a 532 nm Spectra Physics solid-state laser at a power of 2 mW.

Acknowledgment. This research was supported in part by DOE Award No. DE-FG02-07ER46376 and NSF Award No. CBET-0854118.

Supporting Information Available: Selected Raman spectra of the nanotube in Figures 2 and 3 at various degrees of strain, showing G band softening and intensity diminishing. This material is available free of charge *via* the Internet at http://pubs.acs.org.

REFERENCES AND NOTES

1. Gupta, S.; Dharamvir, K.; Jindal, V. K. Elastic Moduli of Single-Walled Carbon Nanotubes and Their Ropes. *Phys. Rev. B* **2005**, *72*, 165428.
2. Wu, Y.; Huang, M. Y.; Wang, F.; Huang, X. M. H.; Rosenblatt, S.; Huang, L. M.; Yan, H. G.; O'Brien, S. P.; Hone, J.; Heinz, T. F. Determination of the Young's Modulus of Structurally Defined Carbon Nanotubes. *Nano Lett.* **2008**, *8*, 4158–4161.
3. Kumar, R.; Cronin, S. B. Optical Properties of Carbon Nanotubes under Axial Strain. *J. Nanosci. Nanotechnol.* **2008**, *8*, 122–130.
4. Sazonova, V.; Yalsh, Y.; Ustunel, H.; Roundy, D.; Arias, T. A.; McEuen, P. L. A Tunable Carbon Nanotube Electromechanical Oscillator. *Nature* **2004**, *431*, 284–287.
5. Chiu, H. Y.; Hung, P.; Postma, H. W. C.; Bockrath, M. Atomic-Scale Mass Sensing Using Carbon Nanotube Resonators. *Nano Lett.* **2008**, *8*, 4342–4346.
6. Lucas, M.; Young, R. J. Effect of Uniaxial Strain Deformation upon the Raman Radial Breathing Modes of Single-Wall Carbon Nanotubes in Composites. *Phys. Rev. B* **2004**, *69*, 85405.
7. Zhao, Q.; Frogley, M. D.; Wagner, H. D. Direction-Sensitive Strain-Mapping with Carbon Nanotube Sensors. *Compos. Sci. Technol.* **2002**, *62*, 147–150.
8. Yakobson, B. I.; Smalley, R. E. Fullerene Nanotubes: C1,000,000 and Beyond. *Am. Sci.* **1997**, *85*, 324.
9. Pugno, N. M. On the Strength of the Carbon Nanotube-Based Space Elevator Cable: From Nanomechanics to Megamechanics. *J. Phys.: Condens. Matter* **2006**, *18*, S1971–S1990.
10. Nardelli, M. B.; Yakobson, B. I.; Bernholc, J. Mechanism of Strain Release in Carbon Nanotubes. *Phys. Rev. B* **1998**, *57*, R4277.
11. Yu, M. F.; Files, B. S.; Arepalli, S.; Ruoff, R. S. Tensile Loading of Ropes of Single Wall Carbon Nanotubes and Their Mechanical Properties. *Phys. Rev. Lett.* **2000**, *84*, 5552.
12. Walters, D. A.; Ericson, L. M.; Casavant, M. J.; Liu, J.; Colbert, D. T.; Smith, K. A.; Smalley, R. E. Elastic Strain of Freely Suspended Single-Wall Carbon Nanotube Ropes. *Appl. Phys. Lett.* **1999**, *74*, 3803–3805.
13. Zhao, Q. Z.; Nardelli, M. B.; Bernholc, J. Ultimate Strength of Carbon Nanotubes: A Theoretical Study. *Phys. Rev. B* **2002**, *65*, 144105.
14. Lucas, M.; Young, R. J. Raman Spectroscopic Study of the Effect of Strain on the Radial Breathing Modes of Carbon Nanotubes in Epoxy/SWNT Composites. *Compos. Sci. Technol.* **2004**, *64*, 2297–2302.

15. Zhao, Q.; Wagner, H. D. Two-Dimensional Strain Mapping in Model Fiber-Polymer Composites Using Nanotube Raman Sensing. *Composites, Part A* **2003**, *34*, 1219–1225.
16. Zhao, Q.; Wagner, H. D. Raman Spectroscopy of Carbon–Nanotube–Based Composites. *Philos. Trans. R Soc. London, Ser. A* **2004**, *362*, 2407–2424.
17. Hadjiev, V. G.; Iliev, M. N.; Arepalli, S.; Nikolaev, P.; Files, B. S. Raman Scattering Test of Single-Wall Carbon Nanotube Composites. *Appl. Phys. Lett.* **2001**, *78*, 3193–3195.
18. Cooper, C. A.; Young, R. J.; Halsall, M. Investigation into the Deformation of Carbon Nanotubes and Their Composites through the Use of Raman Spectroscopy. *Composites, Part A* **2001**, *32A*, 401–411.
19. Schadler, L. S.; Giannaris, S. C.; Ajayan, P. M. Load Transfer in Carbon Nanotube Epoxy Composites. *Appl. Phys. Lett.* **1998**, *73*, 3842–3844.
20. Cronin, S. B.; Swan, A. K.; Unlu, M. S.; Goldberg, B. B.; Dresselhaus, M. S.; Tinkham, M. Measuring the Uniaxial Strain of Individual Single-Wall Carbon Nanotubes: Resonance Raman Spectra of Atomic-Force-Microscope Modified Single-Wall Nanotubes. *Phys. Rev. Lett.* **2004**, *93*, 167401.
21. Cronin, S. B.; Swan, A. K.; Unlu, M. S.; Goldberg, B. B.; Dresselhaus, M. S.; Tinkham, M. Resonant Raman Spectroscopy of Individual Metallic and Semiconducting Single-Wall Carbon Nanotubes under Uniaxial Strain. *Phys. Rev. B* **2005**, *72*, 35425.
22. Kumar, R.; Cronin, S. B. Raman Scattering of Carbon Nanotube Bundles under Axial Strain and Strain-Induced Debundling. *Phys. Rev. B* **2007**, *75*, 155421.
23. Kumar, R.; Aykol, M.; Cronin, S. B. Effect of Nanotube–Nanotube Coupling on the Radial Breathing Mode of Carbon Nanotubes. *Phys. Rev. B* **2008**, *78*, 165428.
24. Brintlinger, T. H. Carbon Nanotube Electronics: Growth, Imaging and Electronic Properties. Ph.D Thesis, University of Maryland, 2005.
25. Sfeir, M. Y.; Wang, F.; Huang, L.; Chuang, C.-C.; Hone, J.; O'Brien, S. P.; Heinz, T. F.; Brus, L. E. Probing Electronic Transitions in Individual Carbon Nanotubes by Rayleigh Scattering. *Science* **2004**, *306*, 1540–1543.
26. Son, H.; Samsonidze, G. G.; Kong, J.; Zhang, Y.; Duan, X.; Zhang, J.; Liu, Z.; Dresselhaus, M. S. Strain and Friction Induced by van der Waals Interaction in Individual Single Walled Carbon Nanotubes. *Appl. Phys. Lett.* **2007**, *90*, 253113.
27. Huang, M. Y.; Wu, Y.; Chandra, B.; Yan, H.; Shan, Y.; Heinz, T. F.; Hone, J. Direct Measurement of Strain-Induced Changes in the Band Structure of Carbon Nanotubes. *Phys. Rev. Lett.* **2008**, *100*, 136803.
28. Dresselhaus, M. S.; Dresselhaus, G.; Jorio, A.; Souza, A. G.; Saito, R. Raman Spectroscopy on Isolated Single Wall Carbon Nanotubes. *Carbon* **2002**, *40*, 2043–2061.
29. Dresselhaus, M. S.; Dresselhaus, G.; Jorio, A.; Souza, A. G.; Pimenta, M. A.; Saito, R. Single Nanotube Raman Spectroscopy. *Acc. Chem. Res.* **2002**, *35*, 1070–1078.
30. Yang, W.; Wang, R. Z.; Yan, H. Strain-Induced Raman-Mode Shift in Single-Wall Carbon Nanotubes: Calculation of Force Constants from Molecular-Dynamics Simulations. *Phys. Rev. B* **2008**, *77*, 195440.
31. Wu, G.; Zhou, J.; Dong, J. Raman Modes of the Deformed Single-Wall Carbon Nanotubes. *Phys. Rev. B* **2005**, *72*, 115411.
32. Gao, B.; Jiang, L.; Ling, X.; Zhang, J.; Liu, Z. Chirality-Dependent Raman Frequency Variation of Single-Walled Carbon Nanotubes under Uniaxial Strain. *J. Phys. Chem. C* **2008**, *112*, 20123–20125.
33. Souza Filho, A. G.; Kobayashi, N.; Jiang, J.; Grüneis, A.; Saito, R.; Cronin, S. B.; Mendes Filho, J.; Samsonidze, G. G.; Dresselhaus, G.; Dresselhaus, M. S. Strain-Induced Interference Effects on the Resonance Raman Cross Section of Carbon Nanotubes. *Phys. Rev. Lett.* **2005**, *95*, 217403.
34. Yang, L.; Han, J. Electronic Structure of Deformed Carbon Nanotubes. *Phys. Rev. Lett.* **2000**, *85*, 154.
35. Tombler, T. W.; Zhou, C.; Alexseyev, L.; Kong, J.; Dai, H.; Liu, L.; Jayanthi, C. S.; Tang, M.; Wu, S.-Y. Reversible Electromechanical Characteristics of Carbon Nanotubes under Local-Probe Manipulation. *Nature* **2000**, *405*, 769–772.
36. Minot, E. D.; Yaish, Y.; Sazonova, V.; Park, J.-Y.; Brink, M.; McEuen, P. L. Tuning Carbon Nanotube Band Gaps with Strain. *Phys. Rev. Lett.* **2003**, *90*, 156401.
37. Maiti, A.; Svizhenko, A.; Anantram, M. P. Electronic Transport through Carbon Nanotubes: Effects of Structural Deformation and Tube Chirality. *Phys. Rev. Lett.* **2002**, *88*, 126805.
38. Cao, J.; Wang, Q.; Dai, H. Electromechanical Properties of Metallic, Quasimetallic, and Semiconducting Carbon Nanotubes under Stretching. *Phys. Rev. Lett.* **2003**, *90*, 157601.
39. Randal, J. G.; Qian, W.; Jien, C.; Dunwei, W.; Hongjie, D. Piezoresistance of Carbon Nanotubes on Deformable Thin-Film Membranes. *Appl. Phys. Lett.* **2005**, *86*, 093104.
40. Maki, H.; Sato, T.; Ishibashi, K. Direct Observation of the Deformation and the Band Gap Change from an Individual Single-Walled Carbon Nanotube under Uniaxial Strain. *Nano Lett.* **2007**, *7*, 890–895.
41. Lee, C.; Wei, X.; Kysar, J. W.; Hone, J. Measurement of the Elastic Properties and Intrinsic Strength of Monolayer Graphene. *Science* **2008**, *321*, 385–388.
42. Liu, F.; Ming, P.; Li, J. *Ab Initio* Calculation of Ideal Strength and Phonon Instability of Graphene under Tension. *Phys. Rev. B* **2007**, *76*, 064120.
43. Hsu, I. K.; Pettes, M. T.; Bushmaker, A.; Aykol, M.; Shi, L.; Cronin, S. B. Optical Absorption and Thermal Transport of Individual Suspended Carbon Nanotube Bundles. *Nano Lett.* **2009**, *9*, 590–594.